HHS Public Access

Author manuscript

Biochemistry. Author manuscript; available in PMC 2020 April 16.

Published in final edited form as:

Biochemistry. 2020 April 14; 59(14): 1442–1453. doi:10.1021/acs.biochem.0c00001.

Subunit Interaction Dynamics of Class Ia Ribonucleotide Reductases: In Search of a Robust Assay

Kanchana Ravichandran[a], **Lisa Olshansky**[a,b], **Daniel G. Nocera**[b], **JoAnne Stubbe**[a,c,*]

[a]Department of Chemistry, Massachusetts Institute of Technology, 77 Massachusetts Avenue, Cambridge, MA 02139

[b]Department of Chemistry and Chemical Biology, Harvard University, 12 Oxford Street, Cambridge, MA 02138

[c]Department of Biology, Massachusetts Institute of Technology, 77 Massachusetts Avenue, Cambridge, MA 02139

Abstract

Ribonucleotide reductases (RNRs) catalyze the conversion of nucleotides (NDP) to deoxynucleotides (dNDP), in part controlling the ratios and quantities of dNTPs available for DNA replication and repair. The active form of *E. coli* class Ia RNR is an asymmetric $\alpha_2\beta_2$ complex in which α_2 contains the active site and β_2 contains the stable diferric-tyrosyl radical cofactor responsible for initiating the reduction chemistry. Each dNDP is accompanied by disulfide bond formation. We now report that β_2 can act catalytically when assaying RNR in either the absence or presence of an external reductant. In the absence of reductant, rapid chemical quench analysis of a reaction of α_2 (10 μM), substrate, and effector with variable amounts of β_2 (0.1, 1 or 10 μM) yields 3 dCDP/α_2 at all ratios of α_2:β_2 with a rate constant of 8–9 s^{-1}, associated with a rate limiting conformational change(s). Stopped-flow fluorescence spectroscopy with a fluorophore-labeled β reveals that the rate constants for subunit association (163 ± 7 μM^{-1} s^{-1}) and dissociation (75 ± 10 s^{-1}) are fast relative to turnover, consistent with catalytic β_2. When assaying in the presence of an external reducing system, the turnover number is dictated by the ratio of α_2:β_2, their concentrations, and the concentration and nature of the reducing system; the

*Corresponding Author: stubbe@mit.edu.

UniProt NUMBERS
E.coli nrdA – P00452
E. coli nrdB – P69924
B. subtilis nrdE – P50620
B. subtilis nrdF – P50621
S. Sanguinis nrdE – A3CLZ6
S. sanguinis nrdF – A3CLZ4
M. tb nrdE – P9WH75
M. tb nrdF – P9WH71
Human RRM1 – P23921
Human RRM2 – P31350

ASSOCIATED CONTENT

Observed dCDP production in the presence of pathway-blocked variants $Y_{356}F$-β_2, and $Y_{731}F$-α_2, previously reported turnover kinetics[14] in the presence of TR/TRR/NADPH, pre-steady state single turnover kinetics of dCDP formation, RNR assays in the presence of optimized endogenous reductant with α:β (1:1) at increasing concentrations. This material is available free of charge via the Internet at http://pubs.acs.org.

rate-limiting step can change from the conformational gating, to a step or steps involving disulfide re-reduction, dissociation of the inhibited $\alpha_4\beta_4$ state or both. The issues encountered in the *E. coli* RNR assays are likely of importance in all class I RNR assays and are central to understand in developing screening assays for inhibitors of these enzymes.

Graphical Abstract

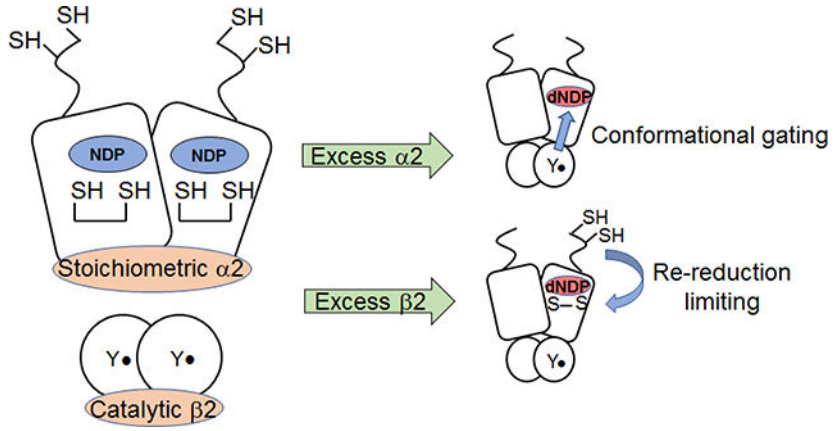

INTRODUCTION

E. coli class Ia ribonucleotide reductase (RNR) catalyzes the conversion of nucleoside 5′-diphosphates (CDP, UDP, GDP, ADP) to their corresponding deoxynucleotides (dNDPs), providing the essential building blocks for DNA replication and repair.[1,2] The *E. coli* Ia enzyme, a paradigm for class I RNRs, consists of two homodimeric subunits, α_2 and β_2, that are active in an asymmetric, tetrameric $\alpha_2\beta_2$ complex.[3–6] The diferric-tyrosyl radical (Y_{122}•) located in β_2 generates a transient thiyl radical in α_2 (C_{439}•) subsequent to its binding NDP and effector, which then initiates NDP reduction. This reversible oxidation process occurs over a distance of ~35 Å and involves a pathway of conserved aromatic amino acid residues and a cysteine.[6,7]

The central role of RNRs in nucleic acid metabolism has made the human RNR the target of five clinically used therapeutics that inhibit distinct steps in the reduction process.[8–10] The limiting factor in identifying new types of RNR inhibitors has been the development of rapid *in vitro* and *in vivo* screens for enzyme activity. In a recent study with an RNR containing a site-specifically incorporated unnatural amino acid, we identified the ability of a mutant β_2 to act catalytically in α_2 turnover.[11] We now report that wt β_2 can also act catalytically in pre-steady state and steady state assays. In support of this result, the kinetics of α/β subunit interactions are fast relative to enzymatic turnover. Consideration of the dynamics of these inter-subunit interactions are important in designing assays for RNR activity and screening for RNR inhibitors.

In early studies to purify *E. coli* RNR,[12] the two subunits separated and required recombination for activity measurement. The K_d for subunit interaction was subsequently established to be 0.4 μM in the apo form and to increase to 0.2 μM on binding of NDP and

its matched allosteric effector.[13] Since that time, RNR subunits have typically been assayed independently, using a physiological concentration of one subunit (0.1–0.5 μM) and a 5 to 10-fold excess of the second subunit to ensure "active" $\alpha_2\beta_2$ complex formation. However, the activity of α_2 is always less than that of β_2,[14] suggesting that the amount of $\alpha_2\beta_2$ complex alone does not govern activity.

RNR assays are typically carried out under two sets of conditions in the absence and presence of endogenous reductant. Our recent model for dNDP formation in the absence of endogenous reducing system (steps A-G) and in its presence (step H) is shown in Scheme 1.[15] Many distinct perturbative biochemical studies and recent structural studies of an active $\alpha_2\beta_2$ double mutant ($F_3Y_{122}/E_{52}Q$-β_2/α_2/GDP/TTP) establish asymmetry within the "active" complex.[15] We propose a model in which α_2, loaded with substrate (CDP) and allosteric effector (ATP), binds to β_2 and that one dCDP is formed in an α/β pair before triggering formation of a second dCDP in the adjacent α/β pair. In the wt enzyme, 2 dCDPs are generated at ~5–10 s^{-1}.[14] In all the perturbative systems examined, the asymmetry becomes apparent as the switching between the two α/β pairs is altered. For the wt system, each dCDP is accompanied by the oxidation of a C_{225},C_{462} pair to a disulfide. The *C*-terminal tail of each α monomer contains two additional conserved cysteines (C_{754}, C_{759}) that are involved in re-reduction of the active site disulfide in their own monomer.[16] While the details of the re-reduction are not established, the structure suggests that the subunits likely dissociate or may undergo a slow conformational reorganization so that two more dCDPs can be generated (step G, Scheme 1) at a rate constant of ~ 0.1 s^{-1}. While a maximum of 4 dCDPs/α_2 can be generated, only 2.5–3 dCDPs are routinely measured. We attribute this observation to α_2's sensitivity to oxidation during its purification and/or handling. Under typical assay conditions for *E. coli* RNR, in the presence of endogenous reductants thioredoxin (TR), thioredoxin reductase (TRR) and NADPH, α_2 generates many dCDPs (step H) with a rate constant of 1–2 s^{-1}, that is likely associated with the complexity of *C*-terminal tail mediated re-reduction and the role of the thioredoxin.[17,18]

Unlike α_2, the Y• in β_2 is regenerated immediately following dCDP formation.[11] This scenario makes it feasible that each β_2 can service multiple α_2s and that fast subunit dissociation and re-association to $\alpha_2\beta_2$ followed by rapid chemistry, could preclude observation of these dynamics. We hypothesize that catalytic β_2 might account for the differences in the turnover number of α_2 and β_2.

In the current study, we describe experiments to examine the ability of β_2 to act catalytically in the absence and in the presence of an external reducing system. In the absence of reductant and at ratios of α:β from 1:1, 10:1 and 100:1, ~3 dCDP/α_2 are generated with a rate constant of 8 s^{-1} relative to $Y^{\bullet}$. When the α:β ratio is 100:1, 200 turnovers occur. Rate constants for association (163 ± 7 μM^{-1} s^{-1}) and dissociation (75 ± 10 s^{-1}) of α_2 and β_2, measured by stopped-flow fluorescence spectroscopy using β_2 modified site-specifically with an environmentally sensitive fluorophore, support a catalytic role for β_2. In the presence of endogenous reductant, we also establish that β_2 can function catalytically. However, under the conditions of limiting α_2 or at high concentrations of the subunits (1 – 10 μM), the rate-limiting step switches from the conformational gating of radical transfer (RT) chemistry to re-reduction of α_2, likely involving conformational change(s)[15] or

interconversion of active and inactive quaternary structures of RNR ($\alpha_2\beta_2$ and $\alpha_4\beta_4$ in *E. coli*)[19] or both.

The observations that (i) β_2 can function catalytically, (ii) the discoveries of the complexity of α's quaternary structures and their dependence on concentration of protein and (deoxy)nucleotides, (iii) incompletely loaded metallocofactor in β, and (iv) the instability of α to oxidation and its propensity to aggregate require consideration when developing assays for both old and new RNRs. These issues lead us to suggest a standard way to assay RNRs that is distinct from the one that has been used for the past few decades.

MATERIALS AND METHODS

Materials

His_6-α_2, specific activity (SA) of 2500 nmol(min-mg)$^{-1}$ and wt-β_2 with 1.2 Y•/β_2, SA of 6000 nmol(min-mg)$^{-1}$ were expressed from the pET28a-*nrdA* and pTB2-*nrdB* plasmids and purified as previously described.[20,21] The diferric-tyrosyl radical in β_2 is always generated by self-assembly,[22] and by our method[23] gives 1.2 Y•s that we believe are unequally distributed between each β_2. Sixty percent of β_2 is active and 40% contains a diferric-center with no radical, is inactive and termed met-β_2. α_2 was pre-reduced prior to use with dithiothreitol (DTT) and treated with hydroxyurea (HU) to reduce the tyrosyl radical in the small amount of β_2 that always co-purifies with α_2.[24] *E. coli* thioredoxin, TR (40 U/mg) and thioredoxin reductase, TRR (1400 U/mg) were purified using established protocols.[25,26] 6-Bromoacetyl-2-dimethylaminonaphthalene (BADAN) was purchased from Molecular Probes (Eugene, OR). $C_{268}S/C_{305}S/V_{365}C$-$\beta_2$ was isolated and labeled with BADAN to make dansyl-β_2 as previously described.[27] For stopped flow (SF) fluorescence spectroscopy experiments, Y_{122}• of wt-β_2 or (dansyl-β_2) was reduced by treatment of β_2 with HU. [5-^{3}H]-CDP was obtained from Vitrax (Placentia, CA). Calf alkaline phosphatase was purchased from Roche. Assay buffer is 50 mM HEPES, 15 mM $MgSO_4$ and 1 mM EDTA (pH 7.6).

dCDP formation kinetics as a function of subunit ratio with no endogenous reductant

Rapid Chemical Quench (RCQ) experiments were performed on a Kintek RQF-3 instrument attached to an external circulating water bath set at 25 °C. To assess the effect of [β_2] on kinetics, wt-α_2 (20 μM) and ATP (6 mM) in assay buffer in syringe A was rapidly mixed with wt-β_2 (0.2, 2 or 20 μM and [5-^{3}H]-CDP (1 mM, 20,000 cpm/nmol) in an equal volume from syringe B. The reaction was quenched in the instrument (5 ms – 100 s) or by hand (> 100 s) in 2% $HClO_4$ and samples were dephosphorylated and worked up as previously described.[14,28] To assess the effect of [$\alpha_4\beta_4$] on dCDP formation kinetics, a control reaction of wt-α_2 (1 μM), wt-β_2 (1 μM), [5-^{3}H]-CDP (0.5 mM) and ATP (3 mM) was also monitored by RCQ. Data were fit to Eq. 1 (for 1:1 and 10:1 α_2:β_2), and Eq. 2 (for 100:1 α_2:β_2) to obtain k_{cat} from the sum of $A_1k_1 + A_2k_2$.

$$y = A_1\left(1 - e^{-k_1 t}\right) + A_2\left(1 - e^{-k_2 t}\right) \quad (1)$$

$$y = A\left(1 - e^{-kt}\right) \quad (2)$$

Association and dissociation rate constants by SF fluorescence spectroscopy

k_{assoc} and k_{dissoc} for the $\alpha_2\beta_2$ complex in the presence and absence of CDP, ATP, and dATP were determined by SF fluorescence spectroscopy using an Applied Photophysics DX.17MV instrument equipped with the Pro-Data upgrade. The temperature was maintained at 22.0 ± 0.1 °C with a Lauda RE106 circulating water bath and all samples were incubated for 3 min at this temperature prior to measurement. Total fluorescence at $\lambda > 420$ nm was detected by a PMT with a long pass filter, using an excitation bandwidth of 40 nm centered at 390 nm. All solutions were prepared in assay buffer. Association rate constants were determined by rapid mixing of 1–6 μM of α_2, ± CDP (0.4 mM), and ± ATP (1.2 mM) in one syringe with an equal volume of 0.16 μM dansyl-β_2 in a second syringe. The reaction was iterated to obtain ~50 traces that were then averaged and fit to Eq. 2 to obtain k_{obs}. Plotting k_{obs} as a function of [α_2] provided k_{assoc} from the slope of the linear fit to Eq. 3 derived from a one-step reversible binding model for pseudo-first order conditions. This process was repeated three times and reported error reported accounts for error between replicates as well as error associated with the goodness of fit.

$$k_{obs} = k_{assoc}[\alpha_2] + k_{dissoc} \quad (3)$$

As determination of k_{dissoc} by extrapolation of Eq. 3 to [α_2] = 0 gives significant error, k_{dissoc} was measured directly by mixing equal volumes of dansyl-β_2 (0.2 μM), α_2 (0.5 μM), ± CDP (0.5 mM) and ± ATP (1.2 mM) or ± dATP (100 μM) in one syringe with a large excess of met-β_2 (100 μM) in a second syringe with the same CDP/ATP. A minimum of 15 traces was averaged per trial and 3–6 independent trials were conducted for each condition (in the presence and absence of CDP and/or ATP). With the exception of dissociation rate constants measured in the presence of dATP, all SF fluorescence traces were well fit to a monoexponential function (Eq. 2) over 1–75 ms. In the presence of dATP, dissociation kinetics were biphasic and fit to Eq. 1 over 0.001–8 s. All fitting was performed using OriginPro 8.0 software (OriginLab). Acceptability of fitting was determined on the basis of qualitative symmetry of residuals about zero amplitude and the R^2 factor.

dCDP formation kinetics as a function of subunit ratio in the presence of TR/TRR/NADPH

RCQ experiments were performed identically to those described above in the absence of reductant with the following minor modifications. Syringe A included TR (80 μM), TRR (1.6 μM) in addition to wt-α_2 (20 μM) and ATP (6 mM), while syringe B contained wt-β_2 (0.2 or 20 μM), [5-^{3}H]-CDP (2 mM, 20,000 cpm/nmol) and NADPH (2 mM). Data were fit to Eq. 4 (for 1:1 and 10:1 α_2:β_2), and Eq. 5 (for 100:1 α_2:β_2) where A and k_{burst} are the amplitude and observed rate constant for the burst phase, respectively, and k_{linear} is the steady-state turnover number (k_{cat}).

$$y = A\left(1 - e^{k_{burst}t}\right) + k_{linear}t \quad (4)$$

$$y = k_{linear}t + c \quad (5)$$

Steady-state turnover kinetics

Assays contained a reaction mixture of 170 μL: wt-α_2 (1–10 μM), wt-β_2 (0.1–10 μM), [5-^{3}H]-CDP (8,000 cpm/nmol, 0.5 mM), ATP (3 mM), TR (40 μM), TRR (0.8 μM) and NADPH (1 mM). Aliquots (40 μL) were quenched at 30 s, 1, 2 and 3 min in 25 μL of 2% $HClO_4$. Product separation was performed as described by Steeper and Steuart.[28]

Kinetics of dimanganese tyrosyl radical RNR (NrdF2-NrdE) with NrdH exogenous reductant

NrdI was purified to homogeneity and used to assemble the dimanganese-tyrosyl radical cofactor in NrdF2. Typically, 0.7 Y•/β were obtained for cluster assembled in NrdF2. In our hands, NrdF1 was always in inclusion bodies. NrdE was purified under a variety of conditions and in all cases its solubility was limited (~10 μM). Full length NrdE, with no tag, was used in these assays. Purification of thioredoxin equivalents (TrxA, TrxB1, Trxc and NrdH) as well as thioredoxin reductase were carried out and examined for activity. NrdH was established to be the physiological reductant.

RESULTS

Effect of catalytic β_2 on inactive site-directed mutants of RNR

Since RNR is essential for *E. coli* viability, over-expression of either mutant α_2 or β_2 always results in small amounts of co-purifying endogenous subunits.[29] For example, Y_{356}F-β_2, a variant incapable of dNDP formation,[30] typically contains between 0.1–5% contaminating wt-β_2. When product formation is examined for a reaction mixture containing 0.34 nmol each of Y_{356}F-β_2 and wt-α_2, CDP, and ATP in the absence of a reducing system, increasing amounts of dCDP are observed with time such that 1.5 dCDP/α_2 are produced within 15 min (Fig. S1). If β_2 is not catalytic with respect to α_2, one would predict that turnover in the absence of a reducing system would result in 0.003–0.15 dCDP/α_2. The observation of a 10–500-fold enhancement over the expected number of dCDPs suggests that one β_2 can service multiple α_2s. In contrast to Y_{356}F-β_2, when similar experiments are performed with another catalytically inactive mutant, Y_{731}F-α_2,[31] only 0.05–0.09 dCDP/α_2 are generated with no visible time dependence. This observation is consistent with 2–3% contaminating wt-α_2 and a non-catalytic role for α_2 with respect to β_2 turnover. These observations together with the observation that α_2 in the presence of excess β_2 vs β_2 in the presence of excess α_2 (Fig. S2) give different turnover numbers provided the impetus for examining the reaction of wt RNR at different α:β ratios.

dCDP formation kinetics as a function of subunit ratio in the absence of reductant

To test the hypothesis that β_2 is catalytic, dCDP was measured at α:β = 1:1, 10:1 or 100:1 (Fig. 1) with 10 μM α_2, and β_2 varied (0.1, 1 or 10 μM). The total amount of dCDP was

normalized per α_2 or Y• and the rate constants calculated from the sum of $A_1k_1 + A_2k_2$ in Eqs. 1 and 2, where A_n and k_n represent the amplitude and rate constant of each kinetic phase (Table 1). As seen in Fig. 1, 2.5–3 dCDP/α_2 are produced at all α:β ratios. At α:β = 1:1 and 10:1, total dCDP production occurs over two kinetic phases: 1.3–1.4 dCDP/α_2 are generated in the first phase and 1.1–1.6 dCDP/α_2 in the second phase. As we previously proposed,[14] the first phase reports on the generation of the first two dCDPs by each α monomer, and the second phase reports on re-reduction of the active site disulfide by the *C*-terminal dithiols of α_2 (Scheme 1). Support for this interpretation is provided by the ability to generate 1.4–1.7 dCDP/α_2 in a single kinetic phase in a mutant α_2 containing serines in place of the *C*-terminal cysteines.[14] At α:β = 100:1, a single kinetic phase producing 2.5 dCDP/α_2 is observed.

In contrast, normalizing product formation relative to equivalents of Y• reveals that a total of 1.1, 10, and 207 dCDP/Y• are formed at α:β = 1:1, 10:1, and 100:1, respectively (Table 1). Recalling that ~60% of β_2 is active and contains 2Y•, the remaining 40% is inactive with only a diferric cluster.[11] Thus, a single active β_2 performs *many* turnovers during the same time α_2 makes 2.5–3 dCDP/α_2 (Fig. 1, Table 1). Calculating the turnover number relative to Y• reveals that product formation occurs at 8–9 s^{-1} in all cases (Table 1). This rate constant is within the 5–10 s^{-1} range reported in previous studies[14] and is associated with the protein conformational gating that occurs prior to initiation of the reaction. As the ratio of α:β increases, the second phase (re-reduction of the α_2 active site) becomes unencumbered by the issues associated by re-reduction of the active site disulfide (Table 1, Scheme 1).

Our previous studies on wt *E. coli* RNR showed that the activity of each subunit in the presence of a 5-fold excess of the second subunit increased with concentration up to 0.5 μM (Fig. S2), but that by 2 μM it decreased by 50%.[14] We recently reported, using size exclusion chromatography analysis, that $\alpha_2\beta_2$ can be converted in part into an inactive $\alpha_4\beta_4$ state at concentrations >10 μM or in the presence of the negative effector dATP.[27] To investigate the potential effects of the $\alpha_4\beta_4$ state on our pre-steady state kinetics measurements, we performed the 1:1 α_2:β_2 experiment at low (1 μM), and high (10 μM) subunit concentrations (Fig. S3, Table 1). No differences were observed in dCDP formation. This result suggests that if $\alpha_4\beta_4$ forms under these experimental conditions that it rapidly reverts back to $\alpha_2\beta_2$.

Measurement of $\alpha_2\beta_2$ subunit association (k_{assoc}) and dissociation (k_{dissoc}) rate constants by stopped-flow fluorescence spectroscopy

For β_2 to function catalytically, dissociation and re-association of the active $\alpha_2\beta_2$ complex must be fast relative to the rate limiting processes. To study this possibility, we prepared β_2 that contains an environmentally sensitive fluorophore site-specifically attached to a cysteine at position 365 within its *C*-terminal tail that is largely responsible for the binding affinity to α_2.[13,30] This dansyl-β_2 exhibits increased fluorescence intensity when the probe is situated in a hydrophobic environment compared to its fluorescence intensity free in buffered solution, providing a method to explore subunit oligomerization.[19,27]

To measure the rate constant for k_{assoc} for $\alpha_2\beta_2$, stopped-flow (SF) fluorescence experiments were performed at varying concentrations of α_2 in > 10-fold excess relative to

dansyl-β_2 (80 nM) for a range of [α_2] (Fig. 2a). The subunits were rapidly mixed and the increases in fluorescence, shown in Fig. 2b, were fit to Eq. 2 for each [α_2]. Plotting the resulting k_{obs} versus [α_2] (Fig. 2c) provided k_{assoc} from a linear fit to Eq. 3. These experiments were performed in the presence and absence of CDP/ATP and yielded k_{assoc} that were similar and range from 150–200 μM^{-1} s^{-1} (Table 2).

Dissociation rate constants (k_{dissoc}) were determined by rapid mixing of α_2(dansyl-β_2) complex (or α_4(dansyl-β_2)$_2$ in the case with 50 μM dATP) with a large excess of wt-β_2 (Fig. 3a). In the absence and presence of CDP and ATP, the loss in fluorescence intensity was fit to a monoexponential decay, Eq. 2, to provide k_{dissoc} values of 75–100 s^{-1} (Fig. 3b, Table 2). k_{dissoc} of the active $\alpha_2\beta_2$ complex is ~8–12-fold faster than the conformational change(s) (8–9 s^{-1}), supporting the proposal that a single β_2 can service multiple α_2s without attenuating turnover kinetics. In contrast, when the experiment is performed in the presence of the inhibitory effector dATP, dissociation kinetics are slow and biphasic (Fig. 3c).

The oligomeric state ($\alpha_2\beta_2$ vs $\alpha_4\beta_4$) of *E. coli* RNR can be controlled by protein concentration and dATP concentrations.[3,19,32,33] We therefore also determined the subunit dissociation rate constant for $\alpha_4\beta_4$ generated in the presence of 50 μM dATP. At these concentrations of dATP, both the specificity and activity sites of α_2 are saturated,[34,35] resulting in a shift toward the inactive $\alpha_4\beta_4$ state.[3,36] Fitting these data to a biexponential decay (Eq. 1), each phase represents ~50% of the total amplitude change and the rate constants obtained are 10- and 100-fold slower than the corresponding dissociation rate constants from the $\alpha_2\beta_2$ complex (Table 2). This is consistent with previous reports of enhanced subunit affinity in the $\alpha_4\beta_4$ state.[19,32] As stated previously, $\alpha_4\beta_4$ formation that may result from high protein concentrations (10 μM of each subunit) does not affect turnover in the absence of TR/TRR/NADPH. However, the slower dissociation kinetics of $\alpha_4\beta_4$ could explain the range of values observed for steady state turnover in the regime where α_2 becomes limiting (Table 3).

Steady state turnover kinetics

Studies by Ge et al. revealed that turnover number of RNR in the presence of TR/TRR/NADPH declines with increasing protein concentration (Fig. S2).[14] With these data, we proposed that the conformational change(s) prior to turnover are rate-limiting under physiological subunit concentrations (0.1–0.5 μM) while some aspect of the re-reduction process governs turnover under higher protein concentrations (1–10 μM). To determine if β acts catalytically in the presence of reductant, standard RNR assays were performed at different concentrations and ratios of α_2 and β_2 (Table 3). In contrast to turnover in the absence of reductant (8–9 s^{-1}), the steady-state turnover varied from 1.4 to 9 s^{-1}. Maximal $\alpha_2\beta_2$ activity with reductant is realized when [α_2] > [β_2]. These data combined with our previous studies[14] provide further support for the catalytic role of β_2 during turnover. Under conditions of α:β = 1:1 and subsequent to complete oxidation of α_2, additional turnovers can only occur upon re-reduction by the TR/TRR/NADPH system. However, in the presence of excess α_2, a single β_2 can “rapidly” dissociate and re-associate with multiple α_2s prior to requirement for re-reduction. Catalytic β_2 could explain the discrepancy between α_2 and β_2 activities as measured by standard assays at physiological concentrations. These data further

suggest that re-reduction is not only rate-limiting during steady-state turnover at high protein concentrations, but also under physiological concentrations when α_2 is limiting.

dCDP kinetics as a function of subunit ratio in the presence of TR/TRR/NADPH

Our previous studies monitoring dCDP formation in the presence of the TR/TRR system with 15 μM α_2 and 32 μM β_2, reported 1.4–1.7 dCDP/α_2 are generated in a burst phase at ~6 s^{-1}, followed by a linear phase reporting on steady-state turnover at 0.9 s^{-1} (Table 4 (top row) and Fig. S2).[14] These experiments provided evidence that re-reduction of α_2 by TR/TRR/NADPH is rate-determining under steady-state turnover at high protein concentrations. Given these results, and the studies above, we predicted that altering the concentration of β_2 in the reaction mixture would not alter the amplitude of the burst phase with respect to α_2, but that it would change when calculated relative to Y•.

RCQ experiments were therefore carried out in the presence of α:β = 1:1 ([α_2] = [β_2] = 10 μM) with the prediction that the burst phase should remain constant with respect to α_2 but minimally double with respect to Y•. We found that 1.9 ± 0.1 dCDP/α_2 and 1.5 ± 0.1 dCDP/Y• (relative to 0.7, see Table 4 top two rows in middle column) are generated in the burst phase at 9 ± 2 s^{-1} (Fig. 4a,). This result is similar to product formation kinetics and stoichiometry in the absence of TR/TRR where β_2 performs several turnovers, servicing all the α_2s prior to re-reduction of the active site disulfide.

Finally, based on our current model, the 8–9 s^{-1} observed rate constant (Table 1) reports on the protein conformational change(s) that gates radical propagation. To support this hypothesis, we measured turnover kinetics in the presence of TR/TRR/NADPH at α:β = 100:1. As shown in Fig. 4b, no burst phase is observed under these conditions. Instead, a linear phase for formation of product with a rate constant of 6.8 ± 0.1 s^{-1} is observed. These results are consistent with the rate-determining step occurring prior to the first turnover.

DISCUSSION

Our studies in 1999 on the adenosylcoblamain (AdoCbl)-dependent *Lactobacillus leichamannii* ribonucleoside triphosphate reductase (RTPR) showing that AdoCbl can act catalytically,[37] were in part, the inspiration for thinking about whether β_2 could function in a similar capacity. The RTPR system lent itself to careful kinetic analysis under two sets of conditions: [AdoCbl] >> [RTPR] and [RTPR] >> [AdoCbl] in the presence of the TR/TRR reducing system. Our studies in the former case revealed that carbon-cobalt bond reformation and AdoCbl dissociation from AdoCbl•RTPR into solution can accompany every turnover, that is the radical chain length of the RTPR catalyzed dNTP reaction is ~1. In that case, the rate-limiting step is disulfide re-reduction by TR/TRR at 2 s^{-1}. Under conditions where [RTPR] >> [AdoCbl], k_{cat} is 15–20 s^{-1} and is governed by the rate constant for AdoCbl dissociation. In this situation, AdoCbl services more than one RTPR, that is, it functions catalytically. The ability of RTPR to release AdoCbl after each turnover can have important implications as previous physiological studies in *L leichamannii* suggested that cells produce RTPR in molar excess of AdoCbl molecules taken into cells. This strategy would thus increase the effective concentration of holo enzyme and enable a higher rate of DNA biosynthesis; elevated levels of RTPR can optimize use of scarce

nutrients such as AdoCbl. The turnover number of 2 s^{-1} is very similar to the turnover number of many class I RNRs (1–2 s^{-1}) when re-reduction occurs by endogenous proteins. Thus, catalytic AdoCbl in the *L leichmannii* class II RNR set a precedent for catalytic β_2 in *E. coli* Ia RNR.

In most cases, the intracellular concentrations of the α and β subunits of class I RNRs have not been measured, although with bacterial systems, where their genes reside in the same operon, it is likely that the α/β ratio is ~1:1. However, as in the case of RTPR, in the class Ia *E. coli* RNR, the availability of the active form of the metallocofactor is carefully controlled based on our studies in which the amount of β_2 was varied genetically and the amount of diferric cluster and tyrosyl radical was measured quantitatively.[38] Future studies will be required to determine not only the amounts of RNR subunits, but the amounts of active, diferric-tyrosyl radical loaded β_2. If future studies reveal that substoichiometric amounts of Y• relative to α_2 is possible, catalytic β_2 could play a physiological role. We note, however, that regardless of the physiological role of catalytic β_2, the ability of *E. coli* RNR to use β_2 catalytically provides an explanation for the differences in activity of α_2 and β_2 under standard assay conditions in which each subunit is assayed in the presence of an excess of the second subunit to form the “same” active complex.

Based on studies of class Ia *E. coli* and human RNRs and class Ib *S. sanguinis*, *B. subtilis*, *M. tuberculosis,* and *E. coli* RNRs, there are important lessons to be learned for performing reliable assays.

(1) Both α and β subunits must be carefully characterized as well as their complexes:

α subunit characterization

α in general is very air sensitive and its oxidation is often irreversible within a few hours if a reductant such as dithiothreitol (DTT) is not always present during purification and protein storage. α is now known to reside in many distinct quaternary structures (monomer, dimer, non-canonical dimer, tetramer, hexamer, fibrils) and the basis for these changes reside, in part in its *N*-terminal, ATP cone domain or partial cone domains.[15] Purification of α is often facilitated by appendage of an *N*-terminal $(His)_6$-tag. An altered N-terminally tagged α must thus be used with caution. The recent availability of $(His)_6$-SUMO-tags, which allows purification by Ni affinity column, followed by complete removal of the tag with the SUMO protease is recommended.[39] The *C*-terminal tail of all αs is always disordered and houses the two essential cysteines required for the re-reduction of the active site disulfide (Scheme 1). Thus, a tag should never be placed at the *C*-terminal end. Anion exchange purification has worked well for all class I RNRs that we have studied. Purification of α in the presence of small molecule reductant and under anaerobic conditions without a tag, might well avoid many problems.

β subunit characterization

β_2 is a homodimer in all class I RNRs and thus quaternary structure is not an issue. The problems routinely encountered with β_2s are the stability of the Y• in the metallocofactor and the quantity of metallocofactor inserted during recombinant expression. First, the tyrosyl radicals of the dimetallo-Y• cofactors have widely varying stability. While the *E. coli* Ia Y•

has a half-life of 4 days at 4 °C, the human enzyme has a half-life of 30 min at 37 °C. Since β is almost always isolated from recombinant sources at an elevated level of expression, it almost never has a full complement of cofactor.[40] Thus, the cofactor must be assembled and characterized with respect to the metal content and Y• per β. The loading of β with 0.5 to 1 Y•/β, from the self-assembly process *in vitro*[22] is distinct from *in vivo* studies[38,41] thus far reported; more basic biology and biochemical studies are required to understand how the cofactors are assembled in cells. In the optimized assembly of the *E. coli* β_2 cofactor, while there are 3.6 irons/β_2, there are typically 1.2 Y•/β_2.[42] Sixty percent of the cluster is the active $Fe^{3+}{}_2$-Y• cofactor and 40% is inactive, tyrosyl radical reduced, $Fe^{3+}{}_2$-YOH. Thus, in most assays that are 1:1 α/β, β_2 always acts catalytically! The cofactor assembly has been optimized for the *E. coli* RNR, but each β_2 is distinct. Since the Y• is a key indicator of activity, optimizing cluster assembly for assays is essential.

α/β complex characterization

Although the α and β subunits in all class I RNRs are structurally homologous, the quaternary structures of α and the α/β complex are unique and appear to be protein concentration- and nucleotide-dependent. While α alone has been found as noted above in many states, it also forms inactive complexes with β ($\alpha_4\beta_4$) in *E. coli*[19] and in a helical α/β fibril in *B. subtilis.*[43] Some have proposed that α_6/β_2 forms exist in *S. cerevisiae* and human RNRs,[44] but in our opinion, the activity of this state is in question. Not much is known about the equilibria of these species and how other factors in cells affect them. Thus, the conditions used to study RNRs must be carefully described.

K_d for subunit interactions

The K_d for subunit interaction is also essential to determine. If the K_d is weak, (0.2 μM) and the protein is diluted during purification or in crude lysates, activity can be lost because the active complex does not form or the subunits dissociate and the active complex cannot reform. An important issue to consider is that K_{dS} are challenging to determine, if one does not understand the quaternary structure of each subunit.

(2) Redox reductants to cycle RNRs for multiple turnovers must be identified:

Given the requirement for re-reduction of the disulfide in α accompanying formation of each dNDP, the endogenous reductant in each organism needs to be determined. DTT is often used to reduce previously unidentified αs because the protein reductant(s) are initially unknown. For this case, the efficiency varies widely and is dependent on the concentration of reductant.[45] As almost all organisms have multiple candidates for α reduction including TR/TRR, glutaredoxin/glutaredoxin reductase/glutathione, NrdH, etc., identification of the most efficient system is very important to obtain the most robust assay for inhibitor(s) discovery.

(3) Assay conditions musts have optimized α:β and reductant ratios:

Knowledge about the RNR and the organism from which it is obtained is a pre-requisite for the best experimental design. Our experiences with class Ia RNRs (*E. coli*, human, and *S. cerevisiae*) and class Ib RNRs (*S. sanquinis*, *B. subtilis,* and *M. tuberculosis*) have suggested

the following general protocol. First, assume that the ratio of α:β is 1:1 and that $\alpha_2\beta_2$ is the active form. We believe this is a reasonable assumption based on the recent structures of an active *E. coli* Ia RNR[15] and structures of *B. subtilis*[43] and *S. typhimurium*[46] Ib RNRs. Second, determine the concentration of RNR in the organism of interest and identify the endogenous reductant. Third, measure the activity of each RNR over the protein concentration range from 0.5 to 5× estimated physiological levels. The results from some recent studies on *S. sanquinis*,[47] *B. subtilis*[39,48] and *M. tuberculosis* dimanganese-tyrosyl radical RNRs using this approach are shown in Fig. S4. The apparent K_m values obtained from these analyses are lower (K_m of 6.4 nM, 0.025 μM, and 0.16 μM, respectively) than a similar experiment with *E. coli* and human Ia RNRs (apparent K_m of 0.2 μM) suggesting "tighter" α/β affinity. However, efforts to isolate active α/β complexes of these Ib RNRs using several biophysical methods (size exclusion chromatography and analytical ultracentrifugation) all revealed that the subunit behavior, as with Ia *E. coli* RNR, is dynamic. Our studies on *M. tb* RNR have shown that it uses a dimanganese-tyrosyl radical cofactor, possesses high activity and behaves similarly to the *B. subtilis* and *S. sanguinis* enzymes, in contrast with the recent report of Fe-loaded NrdF2.[49] In the case of the *B. subtilis* RNR, the assay approach described above appears to avoid the known complexities associated with complex quaternary structure[43] in this system.

(4) The rate limiting steps for single vs multiple turnovers of RNR must be considered:

Studies on *E. coli* Ia RNR have shown that the rate limiting steps for single turnover is described by a rate constant of 8–9 s^{-1} whereas multiple turnovers of RNR yields a rate constant of 1–2 s^{-1}. Thus, experiments on RNR are typically performed under two general conditions: one in the steady state with endogenous reductant and the other under "single" turnover in the absence of a reducing system. In the former case, low protein amounts are sufficient and the protocol described in (3) is recommended in search of small molecule RNR inhibitors. Once an inhibitor is identified, the target of the inhibition (tyrosyl radical reduction in β, active site modification in α, altered quaternary structure of α or α/β, etc.) can be identified using the "single" turnover approach. In this case, elevated levels of protein are required so that the method of analysis can detect a single equivalent or less of intermediate or product.

CONCLUDING REMARKS

We highlight here that studies on newly discovered RNRs must identify the system and describe the assay conditions carefully. Heroic studies are now turning to examining RNR *in vivo* owing to the importance of inhibiting the enzyme for development of antibacterial and anticancer therapies. Considering the complexity of *in vitro* RNR assays, as shown herein for *E. coli* class I RNR, the design of *in vivo* assays[50] for such studies will be extremely challenging. Understanding RNR's properties is important for uncovering its role in nucleotide metabolism in general, and key for development of assays for new RNR inhibitors *in vitro* and *in vivo*.

Supplementary Material

Refer to Web version on PubMed Central for supplementary material.

ACKNOWLEDGEMENT

The authors gratefully the NIH for funding, DGN (GM 47274) and JS (GM 29595) and LO acknowledges the NSF for a graduate fellowship.

ABBREVIATIONS

RNR	class Ia ribonucleotide reductase from *E. coli*
SF	stopped flow
RCQ	rapid chemical quench
TR	thioredoxin
TRR	thioredoxin reductase

REFERENCES

(1). Stubbe J, and van der Donk WA (1998) Protein radicals in enzyme catalysis. Chem. Rev 98, 705–762. [PubMed: 11848913]

(2). Jordan A, and Reichard P (1998) Ribonucleotide reductases. Annu. Rev. Biochem 67, 71–98. [PubMed: 9759483]

(3). Brown NC, and Reichard P (1969) Ribonucleoside diphosphate reductase. Formation of active and inactive complexes of proteins B1 and B2. J. Mol. Biol 46, 25–38. [PubMed: 4902211]

(4). Thelander L (1973) Physicochemical characterization of ribonucleoside diphosphate reductase from *Escherichia coli*. J. Biol. Chem 248, 4591–4601. [PubMed: 4578086]

(5). Minnihan EC, Ando N, Brignole EJ, Olshansky L, Chittuluru J, Asturias FJ, Drennan CL, Nocera DG, and Stubbe J (2013) Generation of a stable, aminotyrosyl radical-induced $\alpha_2\beta_2$ complex of *Escherichia coli* class Ia ribonucleotide reductase. Proc. Natl. Acad. Sci. U.S.A 110, 3835–3840. [PubMed: 23431160]

(6). Uhlin U, and Eklund H (1994) Structure of ribonucleotide reductase protein R1. Nature 370, 533–539. [PubMed: 8052308]

(7). Stubbe J, Nocera DG, Yee CS, and Chang MCY (2003) Radical initiation in the class I ribonucleotide reductase: long-range proton-coupled electron transfer? Chem. Rev 103, 2167–2201. [PubMed: 12797828]

(8). Shao J, Zhou B, Chu B, and Yen Y (2006) Ribonucleotide reductase inhibitors and future drug design. Curr. Cancer Drug Targets 6, 409–431. [PubMed: 16918309]

(9). Cerqueira NMFSA, Pereira S, Fernandes PA, and Ramos MJ (2005) Overview of ribonucleotide reductase inhibitors: an appealing target in anti-tumour therapy. Curr. Med. Chem 12, 1283–1294. [PubMed: 15974997]

(10). Wnuk SF, and Robins MJ (2006) Ribonucleotide reductase inhibitors as anti-herpes agents. Antiviral Res. 71, 122–126. [PubMed: 16621038]

(11). Ravichandran KR, Minnihan EC, Wei Y, and Stubbe J (2015) Reverse electron transfer completes the catalytic cycle in a 2,3,5-trifluorotyrosine-substituted ribonucleotide reductase. J. Am. Chem. Soc 137, 14387–14395. [PubMed: 26492582]

(12). Brown NC, Canellakis ZN, Lundin B, Reichard P, and Thelander L (1969) Ribonucleoside diphosphate reductase. Purification of the two subunits, proteins B1 and B2. Eur. J. Biochem 9, 561–573. [PubMed: 4896737]

(13). Climent I, Sjöberg B-M, and Huang CY (1991) Carboxyl-terminal peptides as probes for *Escherichia coli* ribonucleotide reductase subunit interaction: kinetic analysis of inhibition studies. Biochemistry 30, 5164–5171. [PubMed: 2036382]

(14). Ge J, Yu G, Ator MA, and Stubbe J (2003) Pre-steady-state and steady-state kinetic analysis of *E. coli* class I ribonucleotide reductase. Biochemistry 42, 10071–10083. [PubMed: 12939135]

(15). Greene BL, Kang G, Cui C, Bennati M, Nocera DG, Drennan CL, and Stubbe J (2020) Ribonucleotide reductases (RNRs): structure, chemistry, and metabolism suggest new therapeutic targets. Annu. Rev. Biochem 89, in press.

(16). Mao SS, Holler TP, Yu GX, Bollinger JM, Booker S, Johnston MI, and Stubbe J (1992) A model for the role of multiple cysteine residues involved in ribonucleotide reduction: amazing and still confusing. Biochemistry 31, 9733–9743. [PubMed: 1382592]

(17). Kasrayan A, Birgander PL, Pappalardo L, Regnström K, Westman M, Slaby A, Gordon E, and Sjöberg BM (2004) Enhancement by effectors and substrate nucleotides of R1-R2 interactions in Escherichia coli class Ia ribonucleotide reductase. J. Biol. Chem 279, 31050-–31057. [PubMed: 15145955]

(18). Lou M, Liu Q, Ren G, Zeng J, Xiang X, Ding Y, Lin Q, Zhong T, Liu X, Zhu L, Qi H, Shen J, Li H, and Shao J (2017) Physical interaction between human ribonucleotide reductase large subunit and thioredoxin increases colorectal cancer malignancy. J. Biol. Chem 292, 9136–9149. [PubMed: 28411237]

(19). Ando N, Brignole EJ, Zimanyi CM, Funk MA, Yokoyama K, Asturias FJ, Stubbe J, and Drennan CL (2011) Structural interconversions modulate activity of *Escherichia coli* ribonucleotide reductase. Proc. Natl. Acad. Sci. U.S.A 108, 21046–21051. [PubMed: 22160671]

(20). Minnihan EC, Seyedsayamdost MR, Uhlin U, and Stubbe J (2011) Kinetics of radical intermediate formation and deoxynucleotide production in 3-aminotyrosine-substituted *Escherichia coli* ribonucleotide reductases. J. Am. Chem. Soc 133, 9430–9440. [PubMed: 21612216]

(21). Yokoyama K, Uhlin U, and Stubbe J (2010) Site-specific incorporation of 3-nitrotyrosine as a probe of pK_a perturbation of redox-active tyrosines in ribonucleotide reductase. J. Am. Chem. Soc. 132, 8385–8397. [PubMed: 20518462]

(22). Atkin CL, Thelander L, Reichard P, and Lang G (1973) Iron and free radical in ribonucleotide reductase. Exchange of iron and Mössbauer spectroscopy of the protein B2 subunit of the *Escherichia coli* enzyme. J. Biol. Chem 248, 7464–7472. [PubMed: 4355582]

(23). Bollinger JM Jr, Tong WH, Ravi N, Huynh BH, Edmonson DE, and Stubbe J (1995) Use of rapid kinetics methods to study the assembly of the diferric-tyrosyl radical cofactor of E. coli ribonucleotide reductase. Meth Enzymol 258, 278–303. [PubMed: 8524156]

(24). Seyedsayamdost MR, Xie J, Chan CTY, Schultz PG, and Stubbe J (2007) Site-specific insertion of 3-aminotyrosine into subunit α_2 of *E. coli* ribonucleotide reductase: Direct evidence for involvement of Y730 and Y731 in radical propagation. J. Am. Chem. Soc 129, 15060–15071. [PubMed: 17990884]

(25). Chivers PT, Prehoda KE, Volkman BF, Kim BM, Markley JL, and Raines RT (1997) Microscopic pK_a values of *Escherichia coli* thioredoxin. Biochemistry 36, 14985–14991. [PubMed: 9398223]

(26). Russel M, and Model P (1985) Direct cloning of the trxB gene that encodes thioredoxin reductase. J. Bacteriol 163, 238–242. [PubMed: 2989245]

(27). Hassan AQ, Wang Y, Plate L, and Stubbe J (2008) Methodology to probe subunit interactions in ribonucleotide reductases. Biochemistry 47, 13046–13055. [PubMed: 19012414]

(28). Steeper JR, and Steuart CD (1970) A rapid assay for CDP reductase activity in mammalian cell extracts. Anal. Biochem. 34, 123–130. [PubMed: 5440901]

(29). Aberg A, Hahne S, Karlsson M, Larsson A, Ormo M, Ahgren A, and Sjöberg BM (1989) Evidence for two different classes of redox-active cysteines in ribonucleotide reductase of *Escherichia coli*. J. Biol. Chem 264, 12249–12252. [PubMed: 2663852]

(30). Climent I, Sjöberg B-M, and Huang CY (1992) Site-directed mutagenesis and deletion of the carboxyl terminus of *Escherichia coli* ribonucleotide reductase protein R2. Effects on catalytic activity and subunit interaction. Biochemistry 31, 4801–4807. [PubMed: 1591241]

(31). Ekberg M, Sahlin M, Eriksson M, and Sjöberg BM (1996) Two conserved tyrosine residues in protein R1 participate in an intramolecular electron transfer in ribonucleotide reductase. J. Biol. Chem 271, 20655–20659. [PubMed: 8702814]

(32). Rofougaran R, Crona M, Vodnala M, Sjöberg B-M, and Hofer A (2008) Oligomerization status directs overall activity regulation of the *Escherichia coli* class Ia ribonucleotide reductase. J. Biol. Chem 283, 35310–35318. [PubMed: 18835811]

(33). Funk MA, Brignole EJ, and Drennan CL Disruption of an oligomeric interface prevents allosteric inhibition of *Escherichia coli* class Ia ribonucleotide reductase. (2018) J. Biol. Chem. 293, 10404–10412. [PubMed: 29700111]

(34). Ormö M, and Sjöberg B-M (1990) An ultrafiltration assay for nucleotide binding to ribonucleotide reductase. Anal. Biochem 189, 138–141. [PubMed: 2278383]

(35). Von Döbeln U, and Reichard P (1976) Binding of substrates to *Escherichia coli* ribonucleotide reductase. J. Biol. Chem 251, 3616–3622. [PubMed: 776972]

(36). Zimanyi CM, Ando N, Brignole EJ, Asturias FJ, Stubbe J, and Drennan CL (2012) Tangled up in knots: structures of inactivated forms of *E. coli* class Ia ribonucleotide reductase. Structure 20, 1–10. [PubMed: 22244750]

(37). Licht SS, Lawrence C, C. L., and Stubbe J (1999) Class II ribonucleotide reductases catalyze carbon-cobalt bond reformation on every turnover. J. Am. Chem. Soc 121, 7463–7468.

(38). Hristova D, Wu CH, Jiang W, Krebs C, and Stubbe J (2008) Importance of the maintenance pathway in the regulation of the activity of Escherichia coli ribonucleotide reductase. Biochemistry 47, 3989–3999. [PubMed: 18314964]

(39). Parker MJ, Ailiena, Maggiolo AO, Thomas WC, Kim A, Meisburger SP, Ando N, Boal A,K, and Stubbe J (2018) An endogenous dAMP ligand in *Bacillus subtilis* class Ib RNR promotes assembly of a noncanonical dimer for regulation by dATP. Proc. Natl. Acad. Sci. U.S.A 115, E4594–E4603. [PubMed: 29712847]

(40). Aye Y, and Stubbe J Clofarabine 5′-di and -triphosphates inhibit human ribonucleotide reductase by altering the quaternary structure of its large subunit. Proc. Natl. Acad. Sci. U.S.A 108, 9815–9820. [PubMed: 21628579]

(41). Hristova D, Perlstein DL, Zhang Z, Huang M, and Stubbe J (2006) Determination of the in vivo stoichiometry of tyrosyl radical per beta betá in *Saccharomyces cerevisiae* ribonucleotide reductase. Biochemistry 45, 12282–12294. [PubMed: 17014081]

(42). Bollinger JM (1983) On the chemical mechanism of assembly of the tyrosyl radical-dinulcear iron cluster cofactor of E. coli ribonucleotide reductase. Ph.D. Thesis Massachusetts Institute of Technology, https://dspace.mit.edu/handle/1721.1/12581

(43). Thomas WC, Brooks FP, Burnim AA, Bacik J-P, Stubbe J, Kaelber JT, Chen JZ, and Ando N (2019) Convergent allostery in ribonucleotide reductase, Nat. Commun 10, 2653. [PubMed: 31201319]

(44). Rofougaran R, Vodnala M, and Hofer A (2006) Enzymatically active mammalian ribonucleotide reductase exists primarily as an alpha(6)beta(2) J. Biol. Chem 281, 27705–27711. [PubMed: 16861739]

(45). Mao SS, Johnston M. I. Bollinger, J. M., and Stubbe J (1989) Mechanism-based inhibition of a mutant Escherichia coli ribonucleotide reductase (cysteine-225----serine) by its substrate CDP. Proc. Natl. Acad. Sci. U.S.A 86, 1485–1489. [PubMed: 2493643]

(46). Uppsten M, Färnegårdh M, Domkin V and Uhlin U (2006) The first holocomplex structure of ribonucleotide reductase gives new insight into its mechanism of action. J. Mol. Biol 359, 365–377. [PubMed: 16631785]

(47). Makhlynets O, Boal AK, Rhodes DV, Kitten D, Rosenzweig AC and Stubbe J (2014) *Streptococcus sanguinis* Class Ib Ribonucleotide reductase: High activity with both iron and manganese cofactors and structural insights. J. Biol. Chem 289, 6259–6272. [PubMed: 24381172]

(48). Parker MJ, Zhu X, and Stubbe J (2014) *Bacillus subtilis* class Ib ribonucleotide reductase: High activity and dynamic subunit interactions. Biochemistry 53, 766–776. [PubMed: 24401092]

(49). Hammerstad M, Røhr AK, Andersen NH, Gräslund A, Högbom M, and Andersson KK (2014) The class Ib ribonucleotide reductase from *Mycobacterium tuberculosis* has two active R2F subunits. J. Biol. Inorg. Chem 19, 893–902. [PubMed: 24585102]

(50). Tholander F, Sjöberg BM. (2012) Discovery of antimicrobial ribonucleotide reductase inhibitors by screening in microwell format. Proc. Natl. Acad. Sci. U.S.A 109, 9798–9803. [PubMed: 22665797]

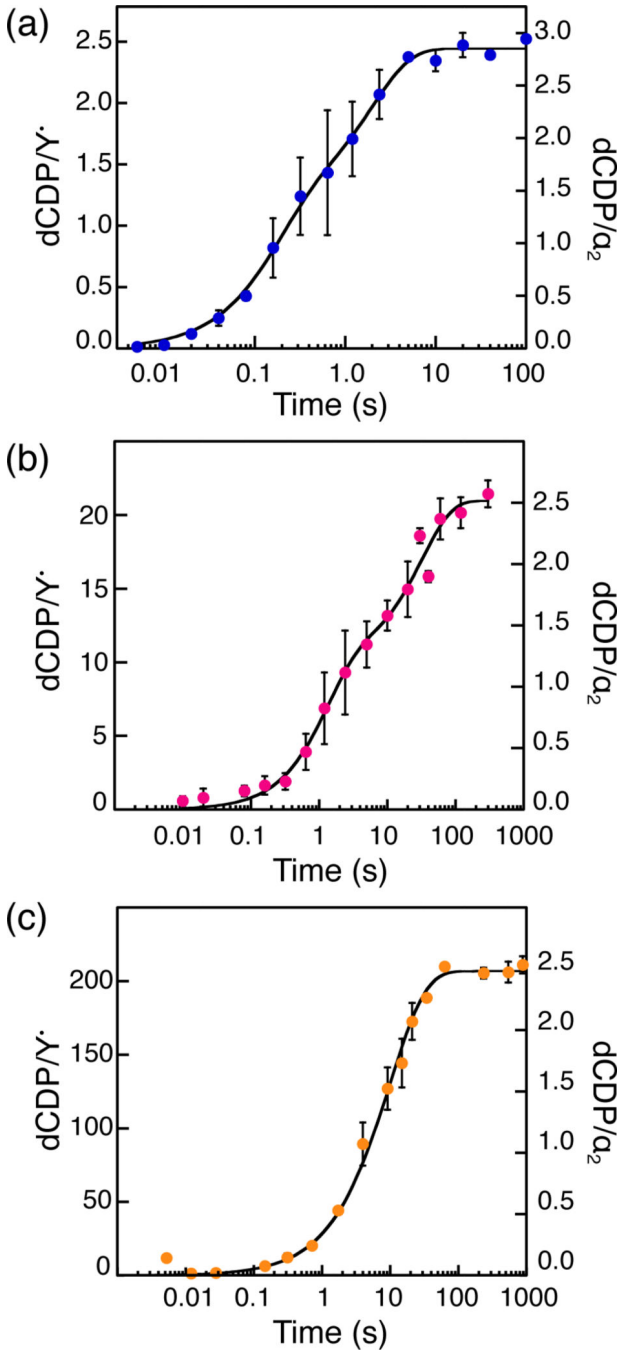

Figure 1.

Product formation kinetics measured by RCQ in the absence of reductant. Final reaction mixtures contained 10 μM α_2, 0.5 mM CDP, 3 mM ATP and (a) 10 μM, (b) 1 μM, or (c) 0.1 μMβ_2 as indicated. Circles and error bars represent the mean and average error of 2 trials, respectively. Black traces represent fits to Eq. 1 (a and b) or Eq. 2 (c) and produced the rate constants and amplitudes listed in Table 1.

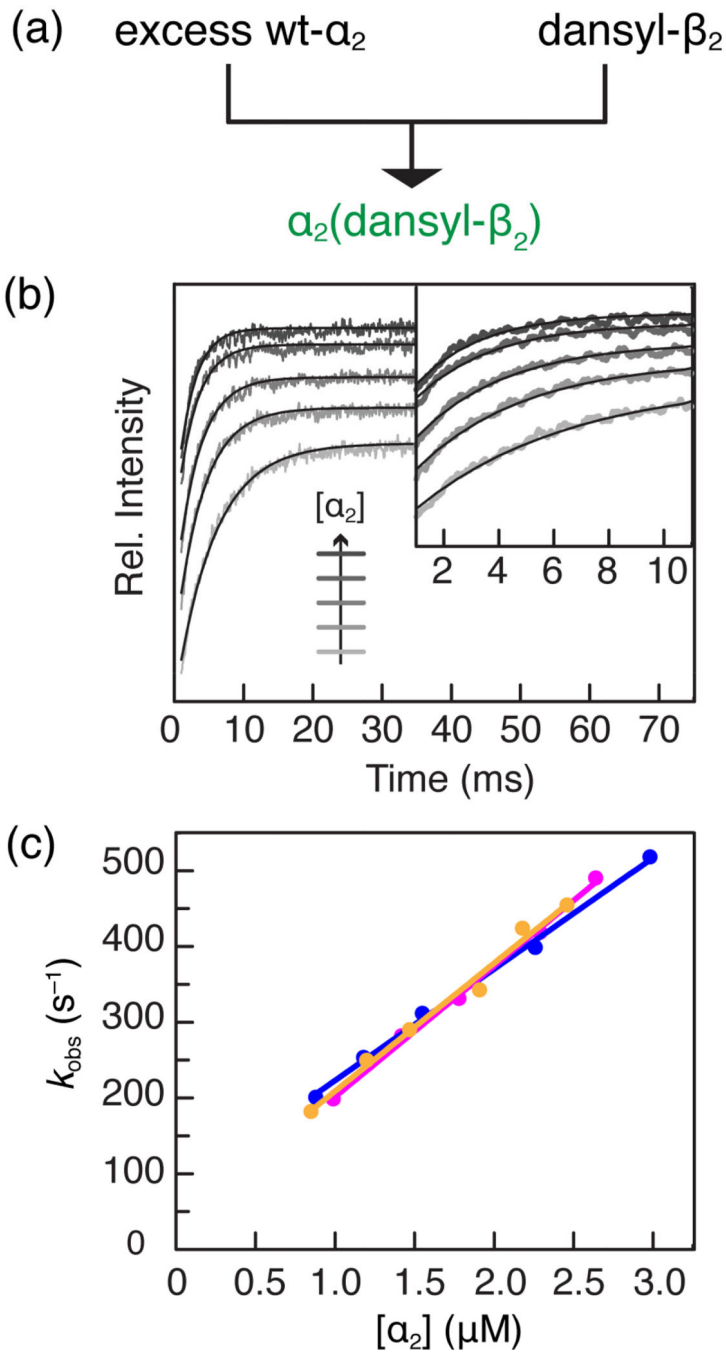

Figure 2.

Diagram describing SF fluorescence experiment to measure (a) k_{assoc}, where green indicates the highly fluorescent state. (b) To extract k_{assoc}, the fluorescence intensity was measured under pseudo-first order conditions for a range of [α_2], and fit to Eq. 2 (black traces, 1 set of 3 data sets shown). (c) k_{obs} (points) obtained in this way were then plotted versus [α_2], and fit (lines) to Eq. 3 to obtain k_{assoc} from the slope of fitted lines.

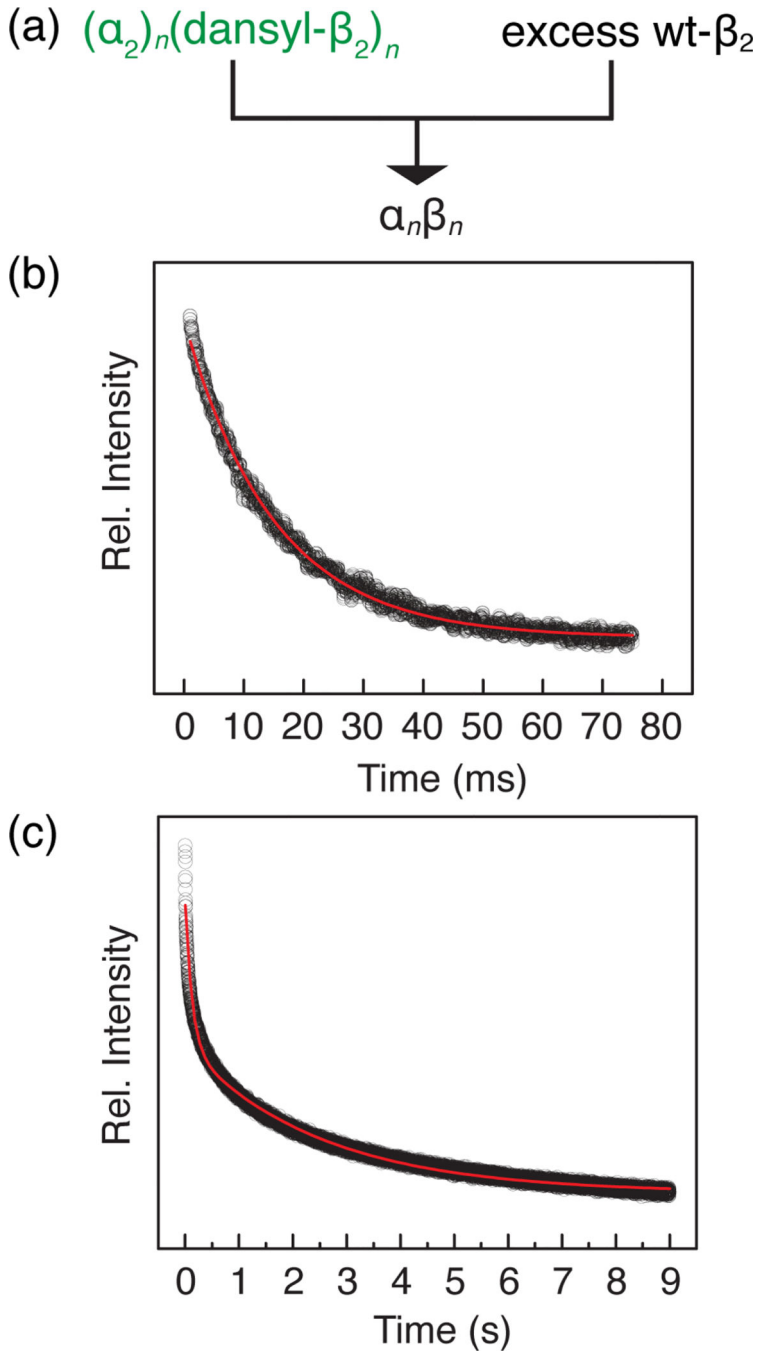

Figure 3.

Scheme for SF fluorescence experiment to determine k_{dissoc} (a), where green indicates the highly fluorescent state and $n = 1$ in (b) and 2 in (c). Fluorescence decay kinetics were measured in the presence of 0.5 mM CDP and 1.5 mM ATP (b), and 50 μM dATP (c). Black circles represent averages of 15 SF traces, and lines are fits to Eq. 2 (b) or 1 (c). The data shown represent 1 of 3 independent trials, the averages and sd of which are presented in Table 2.

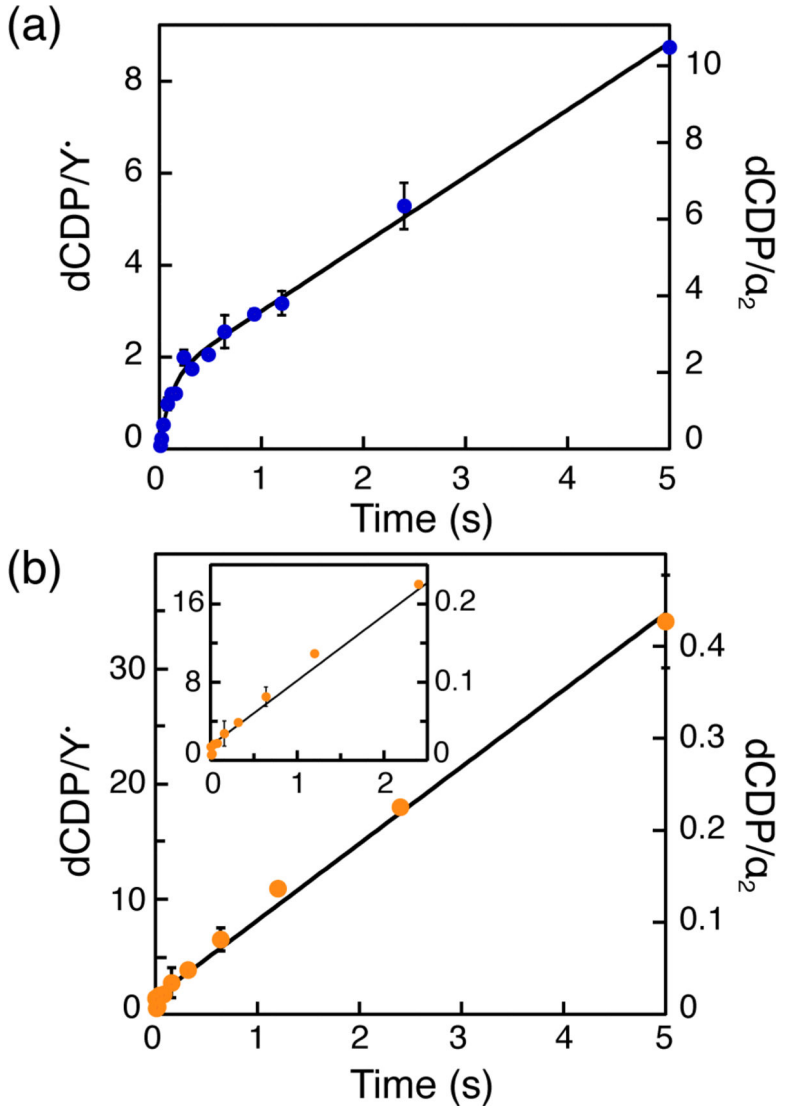

Figure 4.

dCDP formation kinetics measured by RCQ in the presence of TR/TRR/NADPH. Reaction mixtures contained α_2 (10 μM), [5-^{3}H]-CDP (1 mM), ATP (3 mM), TR (40 μM), TRR (0.8 μM), NADPH (1 mM), and β_2 at either 10 μM, (a), or 0.1 μM, (b). Data points represent the averages of two trials. Black traces represent fits to Eq. 4 (a) or 5 (b).

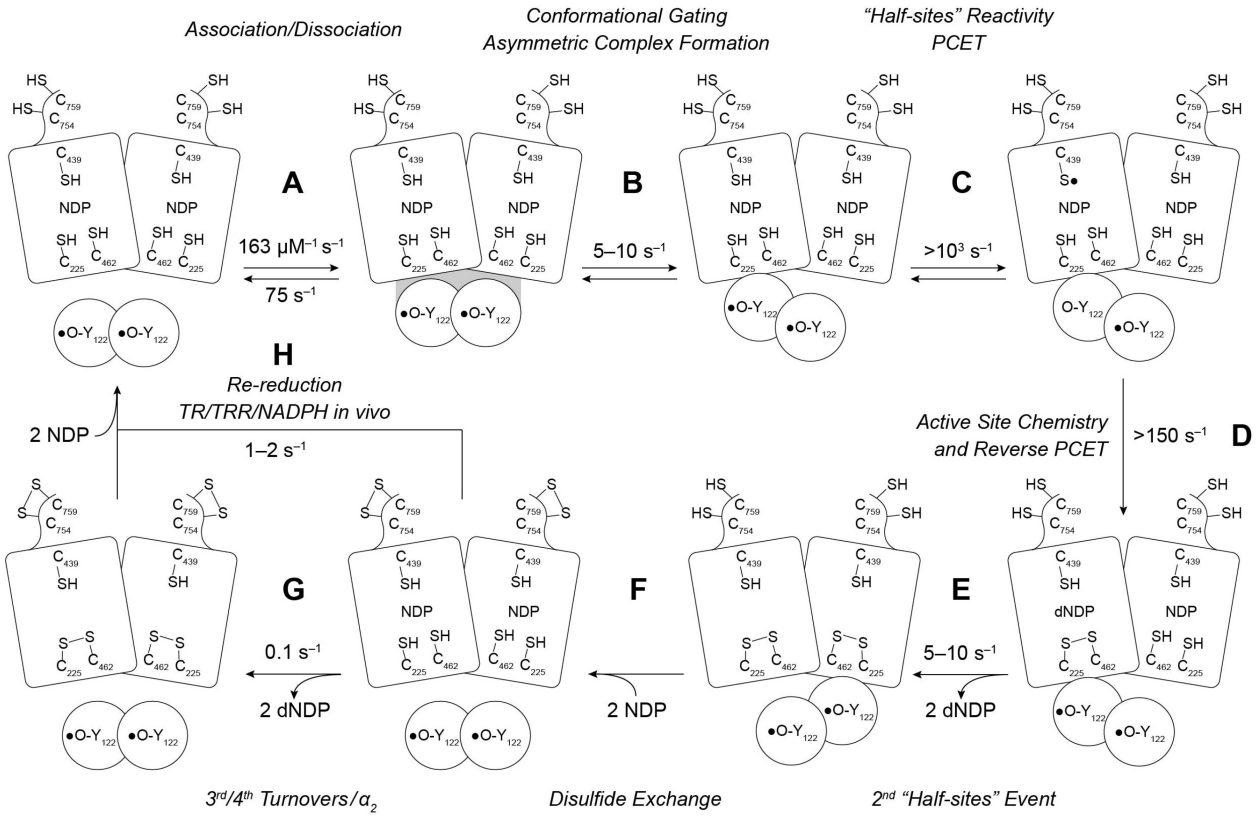

Scheme 1.

Updated model for kinetics of dNDP formation in the absence of endogenous reductant at 5–10 s^{-1} (steps A-G), and in the presence of endogenous reductant and multiple turnovers (step H) at 1–2 s^{-1}.

Table 1.

dCDP formation kinetics at varying ratios of α:β in the absence of reductant.

α_2 (μM)	β_2 (μM)	First phase			Second phase			k_{cat} [b] (s^{-1})
		k_1 (s^{-1})	dCDP/ α_2	dCDP/Y• [a]	k_2 (s^{-1})	dCDP/α_2	dCDP/Y• [a]	
10	10	6 (1)	1.3 (2)	1.1 (1)	0.51 (8)	1.6 (2)	1.3 (1)	8 (1)
10	1	0.8 (2)	1.4 (1)	10 (1)	0.030 (7)	1.1 (1)	11 (1)	8 (2)
10	0.1	0.046 (2)	2.5 (1)	207 (3)	–	–	–	9.5 (4)
1	1	6 (1)	1.5 (2)	1.2 (1)	0.9 (1)	1.5 (2)	1.2 (1)	8 (1)

[a] Y• amount used in the dCDP/ Y• calculation was obtained from the moles of β_2 (87,000 g/mol) in the reaction mixture and the amount of radical per dimer (1.2).

[b] $k_{cat} = A_1 k_1 + A_2 k_2$, where A_n refers to the amplitude with respect to Y•.

Table 2.

Association and dissociation rate constants as a function of CDP and effector measured by SF fluorescence spectroscopy.

Substrate/Effector	k_{assoc} (μM^{-1} s^{-1})	k_{dissoc} (s^{-1})
CDP/ATP	163 (7)	75 (10)
CDP	193 (7)	93 (3)
ATP	156 (14)	86 (10)
None	179 (11)	109 (6)
dATP[a]		0.46 (4), 7 (2)

[a]50 μM, sufficient to saturate both the specificity- and activity-allosteric binding sites.

Table 3.

Steady-state turnover numbers for different α:β ratios.

β_2 (μM)	α_2 (μM)	$\alpha_2\beta_2$ [a] (% β_2 in complex)	k_{cat} [b] (s^{-1})
0.1	10	98	9.0 (3)
1	10	98	7.8 (1)
10	10	96	1.45 (4)
1	1	64	4.3 (2)
0.2 [c]	1	81	6.8 (3)

[a] Assuming a K_d for $\alpha_2\beta_2$ of 0.2 μM (ref 13).

[b] Turnover number in the presence of TR/TRR/NADPH. k_{cat} has not been scaled for the percentage of active complex.

[c] These are our standard assay conditions to assess β_2 activity.

Table 4.

dCDP formation kinetics at varying ratios of α:β in the presence of TR/TRR/NADPH.

[α_2] (μM)	[β_2] (μM)	Burst phase			Linear phase	
		k_{burst} (s^{-1})	dCDP/α_2	dCDP/Y•	k_{cat}/α_2 (s^{-1})	k_{cat}/Y• (s^{-1})
15	32[a]	6.1	1.4	0.7	0.9	–
10	10[b]	9 ± 2	1.9 ± 0.1	1.5 ± 0.1	1.85 ± 0.05	1.45 ± 0.04
10	0.1[b]	–	–	–	–	6.8 ± 0.08

[a]Adapted from reference 14, 0.9 Y•/β_2.

[b]Current work, 1.2 Y•/β_2.